

$n$  = number density  
 $P$  = pressure  
 $P_o(n)$  = pressure of homogeneous fluid at density  $n$   
 $R$  = gas constant  
 $T$  = temperature  
 $u$  = intermolecule potential  
 $V$  = volume  
 $x$  = distance

#### Greek Letters

$\alpha$  = Peng-Robinson parameter  
 $\nabla$  = gradient operator  
 $\gamma$  = surface tensions  
 $\epsilon$  = energy parameter  
 $\omega$  = grand thermodynamic potential  
 $\omega_a$  = eccentric factor  
 $\sigma$  = length parameter  
 $\mu$  = chemical potential

#### Superscripts and Subscripts

$B$  = bulk  
 $C$  = critical  
 $g$  = gas  
 $l$  = liquid  
 $R$  = reduced  
 $+$  = density independent  
 $o$  = homogeneous fluid property  
 $\bullet$  = dimensionless

#### LITERATURE CITED

- Abrams, D. S., and J. M. Prausnitz, "Statistical Thermodynamics of Liquid Mixtures: A New Expression for the Excess Gibbs Energy of Partly or Completely Miscible Systems," *AIChE J.*, **21**, 116 (1975).  
 Bongiorno, V., and H. T. Davis, "Modified Van der Waals Theory of Fluid Interfaces," *Phys. Rev.*, **A12**, 2213 (1975).  
 Bongiorno, V., L. E. Scriven, and H. T. Davis, "Molecular Theory of Interfaces," *J. Col. Int. Sci.*, **57**, 462 (1976).  
 Horvath, A. L., "Redlich-Kwong Equation of State: Review for Chemical Engineering Calculations," *Chem. Eng. Sci.*, **29**, 1334 (1974).  
 Peng, D. Y., and D. B. Robinson, "A New Two Constant Equation of State," *Ind. Eng. Chem. Fundamentals*, **15**, 59 (1976).  
 Reif, F., *Fundamentals of Statistical and Thermal Physics*, McGraw-Hill, New York (1965).  
 Salter, S. J., and H. T. Davis, "Statistical Mechanical Calculations of the Surface Tension of Fluids," *J. Phys. Chem.*, **63**, 3295 (1973).  
 Toxvaerd, S., "Perturbation Theory for Nonuniform Fluids: Surface Tension," *J. Chem. Phys.*, **55**, 3116 (1971).  
 Wilson, G. M., "Areas of Research on Activity Coefficients from Group Contributions at the Thermochemical Institute," in *Phase Equilibria and Fluid Properties in the Chemical Industry*, T. S. Storvick and S. I. Sandler, ed., ACS Symposium Series 60 (1977).

Manuscript received October 14, 1977; revision received June 5, and accepted June 21, 1978.

# Time Resolution of Rapid Processes Using Numerical Calculation and Inversion of Laplace Transforms

W. A. HAHN

and

J. O. L. WENDT

Department of Chemical Engineering  
 University of Arizona  
 Tucson, Arizona 85721

A method for the interpretation of data which results from a signal altered by a process of known weighting function was developed. The method is based on the numerical evaluation and inversion of the Laplace transform. For two different weighting functions, it is shown how narrow a signal can be interpreted accurately. The method is then applied to coal volatilization data.

## SCOPE

In many chemical engineering problems, a rapid process can be experimentally followed by a detector, only after some (known) distortion of the signal has occurred. The

effect of the distortion is to retard and broaden the time span measured, thus allowing for a finite detector response. This paper is concerned with numerical procedures that allow recovery of a signal (input) which has been distorted by a process with a known transfer function and where the

0001-1541-78-1732-1080-\$00.95. © The American Institute of Chemical Engineers, 1978.

output of the process is the measured quantity. Given an experimental output and a known transfer function, the input is determined by dividing the Laplace transform of the measured detector response by the transfer function and inverting the result. A central feature of this paper is that the Laplace transforms are both obtained and inverted numerically, and a comparison of numerical techniques of Bellman (1966) and of Krylov (1969) is obtained.

The purpose of the present work was to determine, quantitatively, the degree to which this method utilizing Laplace transforms could be implemented in practice. Specifically, we determine how narrow an input could be obtained, with accuracy, for two transfer functions and for given outputs. Clearly, numerical inaccuracies do not allow determination of a delta function as an input from the appropriate output.

A methodology for determining practical limits of this approach was developed. First, a Gaussian distribution was convoluted (in the time domain) with the appropriate weighting function. The output so obtained was numerically transformed into the Laplace space, and the resulting input was recalculated using both numerical inversion techniques. Accuracy of the recalculated input was determined by comparison with the original signal. Two

different weighting functions used in this work corresponded to a single well-stirred tank and to a well-stirred tank followed by axial dispersion in a capillary (with a time lag). Although practical limits of this method, and necessary precautions to be taken, do depend on the weighting functions used, the methodology described herein can be employed to determine the value of this method for other weighting functions.

Numerical inversion of Laplace transforms is not new (Seinfeld and Lapidus, 1974). Previous work has utilized Bellman's method (Sy and Lightfoot, 1971) and Krylov's method (Hahn and Plachco, 1977) for the solution of specific equations. Laplace transforms are traditionally used to determine transfer (and/or weighting functions) from known inputs and outputs. This work is different in that we wish to determine a distorted input from a known transfer function and from numerical output data, and indeed we wish to investigate how narrow an input can be detected (in practice) using numerical evaluation and inversion of Laplace transforms. This paper should, therefore, be viewed as a practical application of available techniques to a new problem, and an important feature of this work is a quantitative comparison of two different inversion techniques.

## CONCLUSIONS AND SIGNIFICANCE

Actual time resolved data, describing coal volatilization in a system in which very severe distortion of the desired signal had occurred, was successfully recovered. In addition, the practical limits of utility of this method were explored.

The advantage of the method described herein is that discrete output data can be interpreted with no a priori knowledge of the input or of input characteristics. The method, however, has a practical limitation in that there is a minimum difference between weighting function and output which can be resolved. When the distortion produces no time lag, very narrow inputs, almost approximating a delta function, can be resolved. This is because at  $t = 0$  there is a significant difference between output and weighting functions. When a time lag is present, the method may be restricted to cases in which the ratio of

heights of the output to that of the weighting function is greater than 1.1, and the ratio of times at which their respective peaks occur is greater than 0.8. Furthermore, special precautions outlined in this paper must be taken, lest noise in the output be interpreted as imaginary input.

Of the two numerical inversion techniques examined here, that of Krylov is to be preferred because it allows the input to be calculated at any chosen time. Bellman's technique, although simpler, can lead to substantial scatter in the predictions, and can overlook, completely, inputs occurring at small times.

General applicability of this method will depend somewhat on the weighting functions used. The methodology described herein can be utilized to determine limits of application for other specific weighting functions.

---

In the acquisition of data of very rapid processes, two major problems are likely to occur. The data to be measured are distorted by some portion of the equipment or the signal is too fast to be measured. In this second case, the signal has to be spread out in time, and the result from this process is measured. In both cases, the informa-

tion available is a function which is related to the signal of interest through convolution with a weighting function. A specific example of such a problem is shown in Figure 1.

The apparatus in Figure 1 was designed to study the evolution of volatiles from a coal particle which was heated very rapidly. The volatiles were quenched by a stream of

cold helium gas blown over the surface of the particle. The helium carries the volatiles through a capillary tube to a detector which measures the concentration of the volatiles as a function of time. The flow rate of the helium was kept small in order to avoid total loss of detector signal due to dilution, and so in the capillary tube there exists a well-defined laminar velocity profile, and diffusion plays a very important role. Also, the effect of diffusion is to spread the signal out in time so that the detector is able to react and give a response different from a single sharp peak. Therefore, the signal measured in the detector was much broader than that corresponding to the actual events at the particle surface.

The problem was, then, to relate the signal measured at the exit of the capillary tube (output signal) to the actual rate of evolution of the species from the particle surface (input signal). The problem is described mathematically by a PDE with a final condition, and its solution using analytical or standard numerical techniques is difficult.

One approach, shown in Figure 2a, to reduce the data is to use a mechanistic model for the physical phenomena that occur inside the particle when it is heated. This model generates an output signal which depends on a number of parameters contained in the model. A nonlinear regression technique can be used to adjust parameters in the model until the output  $[O(t)]$  agrees with experimental data. This method has been applied successfully by Blair et al. (1977), but the shape of the input  $I(t)$  is restricted by the choice of the model.

A second approach, shown in Fig. 2b, is to use nonlinear regression to adjust a set of parameters which represent points of the input signal. This approach was attempted in this work, using a modified Marquardt algorithm (Marquardt, 1963), but it failed because the nonlinear regression diverged.

A third approach, shown in Fig. 2c, takes into account that there is a relation between the Laplace transform of the input and the Laplace transform of the output. Namely, the Laplace transform (LT) of the output equals the LT of the input times the LT of the weighting function. Thus, the LT of the input can be obtained without recurrence to a model, and this allows information (such as the shape of the input) needed to develop the physical model to be obtained. The LT of discrete data output may be obtained by direct numerical integration. Once the LT of the input function has been obtained, it must be inverted to yield the actual signal as a function of time. This can be accomplished by numerical techniques.

The present study shows how and to what accuracy this approach may be implemented. This was done by choosing an input function and calculating, by convolution in the time domain, the output that would be obtained from equipment which has a given weighting function. Then this output was transformed and divided by the transform of the weighting function (transfer function), thus yielding the transform of the input. This transform was inverted numerically using two different techniques, and the result was compared to the initial input. Finally, it is shown how the method was used to reduce actual data from coal volatilization as obtained in the apparatus shown in Figure 1.

#### NUMERICAL INVERSION AND EVALUATION OF THE LAPLACE TRANSFORM

There exist two fundamentally different techniques for the numerical inversion of a Laplace transform. These techniques are both based on numerical quadrature to evaluate an integral. The technique developed by Krylov

and Skoblya (1969) is based on numerical calculation of the integral involved in the inversion theorem

$$f(t) = \frac{1}{2\pi i} \int_{c-i\infty}^{c+i\infty} e^{pt} F(p) dp \quad (1)$$

while the technique developed by Bellman, Kalaba, and Lockett (1966) and Bellman et al. (1964) uses numerical quadrature on the integral which defines the Laplace transform:

$$F(p) = \int_0^\infty e^{-pt} f(t) dt \quad (2)$$

Both methods require that the function  $F(p)$  be evaluated for certain values of the complex variable  $p$ .

The principal advantage of Bellman's method is that  $p$  is chosen to be a real number, and no complex arithmetic is involved in the application of this inversion technique; however, the values of the inverse function are obtained at fixed points in time, and the freedom to choose a particular time interval of interest is lost. Krylov's technique involves complex arithmetic, but the time at which the inverse is obtained is a parameter and can be chosen arbitrarily.

The fact that for Krylov's method the value of  $p$  is a complex number makes the numerical evaluation of  $F(p)$  difficult in that normal quadrature formulas cannot be used. If the variable  $p$  is expressed as

$$p = x + iy \quad (3)$$

Equation (2) after some rearrangement becomes

$$F(p) = \int_0^\infty e^{-xt} \cos(yt) f(t) dt - i \int_0^\infty e^{-xt} \sin(yt) f(t) dt \quad (4)$$

The integrands in Equation (4) show an oscillatory behavior with frequency  $y$ . Krylov's technique requires this frequency to be very high, and so the integrals to be evaluated require use of Filon's quadrature (Filon, 1928).

#### STATEMENT OF THE PROBLEM

It was desired to develop a methodology that allowed the practical limits of the numerical Laplace transform method to be determined. Specifically, we wished to determine the smallest difference between an output and a weighting function that could be numerically evaluated in terms of a narrow input function. Clearly, numerical inaccuracies do not allow accurate determination of a delta function as an input, where the output is identical to the weighting function. Furthermore, it is evident that there exist pairs of outputs and weighting functions for which no inputs exist; that is, the input is imaginary and may lie on the negative time axis.

The methodology developed here consisted of the following. First, a normal distribution with adjustable variance  $\sigma$

$$I(t) = \frac{1}{\sqrt{2\pi}\sigma} \exp [-(t - \bar{t})^2 / 2\sigma^2] \quad (5)$$

was chosen as the known input. As  $\sigma$  approaches zero,  $I(t)$  approaches a delta function. This input was convoluted with the weighting function, to be defined subsequently, to obtain the output as a function of time. This output was transformed numerically into Laplace space, divided by the transfer function, and the result inverted to yield the recalculated input. The latter was compared to the original normal distribution. This procedure was

continued for decreasing values of  $\sigma$  until a minimum value of  $\sigma$  was found, below which a stable solution was unobtainable. Results shown are from programs in double precision on a D4C-10 computer, that is, utilizing a capability of carrying fifteen significant figures.

In this work, two different weighting functions were used, the first one being the weighting function associated with a well-stirred tank. This weighting function was chosen because it produces a smooth output with no time lag. The second weighting function is the one corresponding to a well-stirred tank followed by axial dispersion in a capillary tube. This weighting function originates an output with a time lag and sometimes a very steep initial slope; it was chosen because it is the weighting function associated with the actual experimental equipment shown in Figure 1. For brevity, the first weighting function will be called "simple weighting function" and the second the "realistic weighting function."

#### Simple Weighting Function

In the time domain, the expression is

$$W(t) = \frac{1}{\tau_1} e^{-t/\tau_1} \quad (6)$$

and its transformed expression is

$$W(p) = \frac{1}{p\tau_1 + 1} \quad (7)$$

The analytic output can be found by convoluting Equation (5) and the weighting function Equation (6); the resulting expression is

$$O(t) = \frac{1}{2\tau_1} \exp\left[\frac{2\bar{t}\tau_1 + \sigma^2}{2\tau_1^2}\right] \left[ \operatorname{erf}\left(\frac{t}{\sqrt{2}\sigma}\right) - \frac{\bar{t}\tau_1 + \sigma^2}{\sqrt{2}\tau_1\sigma} \operatorname{erf}\left(\frac{\bar{t}\tau_1 + \sigma^2}{\sqrt{2}\tau_1\sigma}\right) \right] e^{-t/\tau_1} \quad (8)$$

In this work we set

$$\tau_1 = 2.04 \text{ s}$$

leading to a weighting function duration of approximately 11 s.

Figure 3 shows the input, weighting function, and output in the time domain for input  $\sigma = 0.2$  s. Figure 3 also defines the quantities  $\alpha$  and  $\beta$ , which are a measure of the differences between the output and weighting functions.

#### Realistic Weighting Function

The weighting function in this case is given by convolution integral of the individual weighting functions of the well-stirred tank and the capillary tube with axial dispersion. The expression of the weighting function in the time domain is given by

$$W(t) = \frac{1}{2\tau_1} \exp\left[D_N \left(\frac{\tau_2}{\tau_1}\right)^2 + \frac{\tau_2}{\tau_1}\right] \left[ \operatorname{erf}\left(\frac{t}{2\tau_2\sqrt{D_N}} - \sqrt{D_N} \frac{\tau_2}{\tau_1} - \frac{1}{2\sqrt{D_N}}\right) - \operatorname{erf}\left(-\sqrt{D_N} \frac{\tau_2}{\tau_1} - \frac{1}{2\sqrt{D_N}}\right) \right] e^{-t/\tau_1} \quad (9)$$

where  $D_N = D_e/\bar{u}L$ . The LT of this weighting function was found in the literature (Wen and Fan, 1975) and

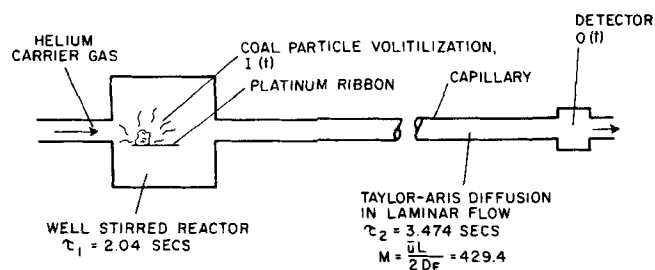
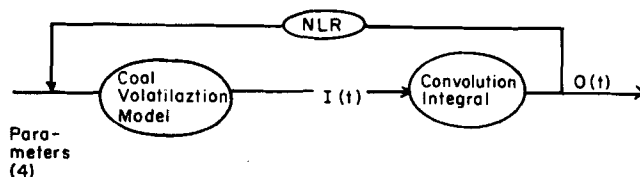
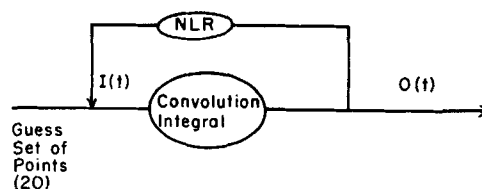


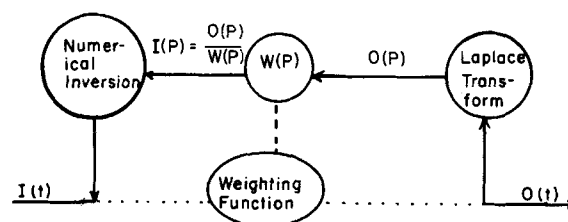
Fig. 1. Schematic of apparatus utilized to obtain coal volatilization data.



#### A: Mechanistic Approach



#### B: Empirical Approach



C: Use of Laplace Transform; Note:  $I(P) = \mathcal{L}[I(t)]$   
 $W(P) = \mathcal{L}[W(t)]$   
 $O(P) = \mathcal{L}[O(t)]$

Fig. 2. Some schemes to analyze distorted data.

is given by

$$W(p) = \frac{e^{M(1-\beta_1)}}{(1-\delta)p\theta + \frac{1+\beta_1}{2}} \quad (10)$$

where

$$\beta_1 = \sqrt{1 + 2\delta p\theta/M} \quad (11)$$

$$\theta = \tau_1 + \tau_2 \quad (12)$$

$$\delta = \tau_2/\theta \quad (13)$$

$$M = \frac{\bar{u}L}{2D_e} = \frac{1}{2D_N} \quad (14)$$

In this work we set

$$\tau_1 = 2.04 \text{ s}$$

$$\tau_2 = 3.474 \text{ s}$$

$$M = 427.4$$

because these values correspond to the actual equipment used (Figure 1).

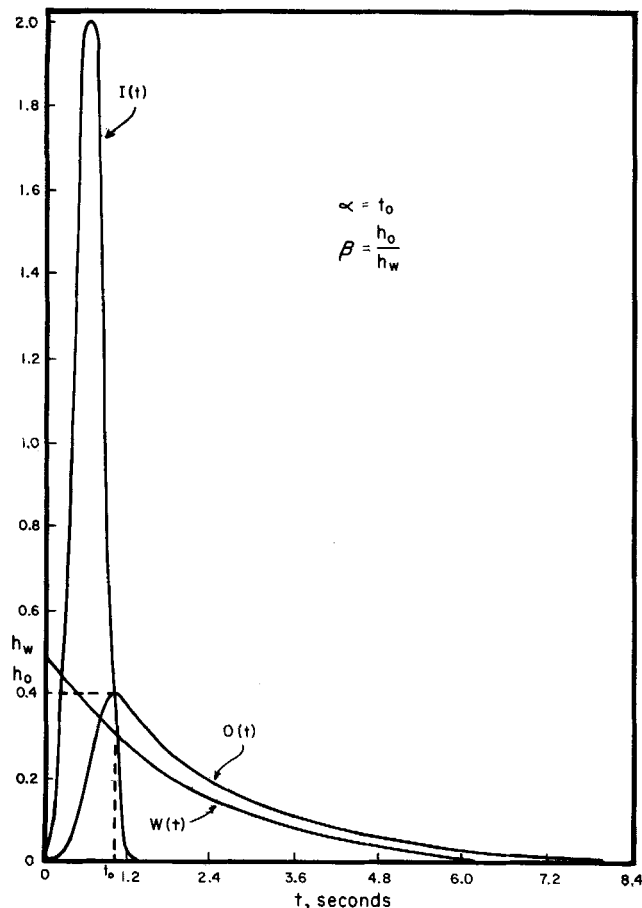


Fig. 3. Input, simple weighting function, and output [Equations (5), (6), and (8)]. Input  $\sigma = 0.2$  s.

It is important to note that Equation (10) is valid only for large values of  $M$ . For this weighting function, the convolution integral which expresses the output was calculated numerically using Gaussian quadrature. Figure 4 shows the input, realistic weighting function, and output in the time domain for input  $\sigma = 0.2$  s. Figure 4 also defines  $\beta$  and  $\gamma$ , both of which are a measure of the difference between output and weighting functions.

In this work, the Laplace transform of the output was obtained by direct numerical integration. When very few data points are available and the shape of the output function is well known, a multiparameter function with known analytic transform can be fitted to this output. Advantages and problems with this latter approach are described by Hahn (1977).

## RESULTS

### Simple Weighting Function

The Laplace transform of the function expressed by Equation (8) was calculated numerically using Gaussian quadrature when  $p$  was a real number (required for Bellman's technique) and using Filon (1928) quadrature when  $p$  was a complex number (required for Krylov's technique). Figure 5 shows results using Krylov's and Bellman's inversion techniques for an input  $\sigma = 0.05$  s,  $\alpha = 0.3$  s,  $\beta = 0.93$ . With Krylov's inversion technique, the agreement between the given and recalculated inputs is perfect. If we use Bellman's inversion, a good, but not perfect, agreement is obtained. Figure 6 shows the results calculated using only Krylov's technique for input  $\sigma = 10^{-6}$  s,  $\alpha = 7 \times 10^{-6}$  s,  $\beta = 1.00$ . It can be observed that the recalculated input still agrees perfectly with the given input. Bellman's method could not be applied be-

cause none of the points in time at which the inverse is calculated corresponds to the period during which the input is different from zero. The good result obtained using Krylov's method shows that an input which is very close to a Dirac function can be obtained. It should be noted, however, that for this weighting function, even a small perturbation to a Dirac function leads to a large perturbation to the weighting function as  $t$  tends to 0, even though  $\beta \approx 1$  and  $\alpha \approx 0$ .

In this case, Krylov's seems to be the better inversion method. It not only permits analysis of much faster signals than Bellman's, but it also leads to much more accurate results.

### Realistic Weighting Function

The output was generated by numerically convoluting Equations (9) and (5).

Figure 7 shows the recalculated input using Krylov's and Bellman's methods for an input  $\sigma = 0.35$  s,  $\beta = 1.21$ ,  $\gamma = 0.76$ . The function obtained using Krylov's method agrees well with the given input, as do some of the points calculated using Bellman's method. For input  $\sigma < 0.35$  s, the scatter in Bellman's points becomes intolerable. Therefore, an input  $\sigma = 0.35$  s is the limit for Bellman's method for this weighting function. Figure 8 shows the input function recalculated using Krylov's method for an input  $\sigma = 0.2$  s,  $\beta = 1.09$ ,  $\gamma = 0.84$ , where agreement with the given input has deteriorated somewhat. For input  $\sigma <$

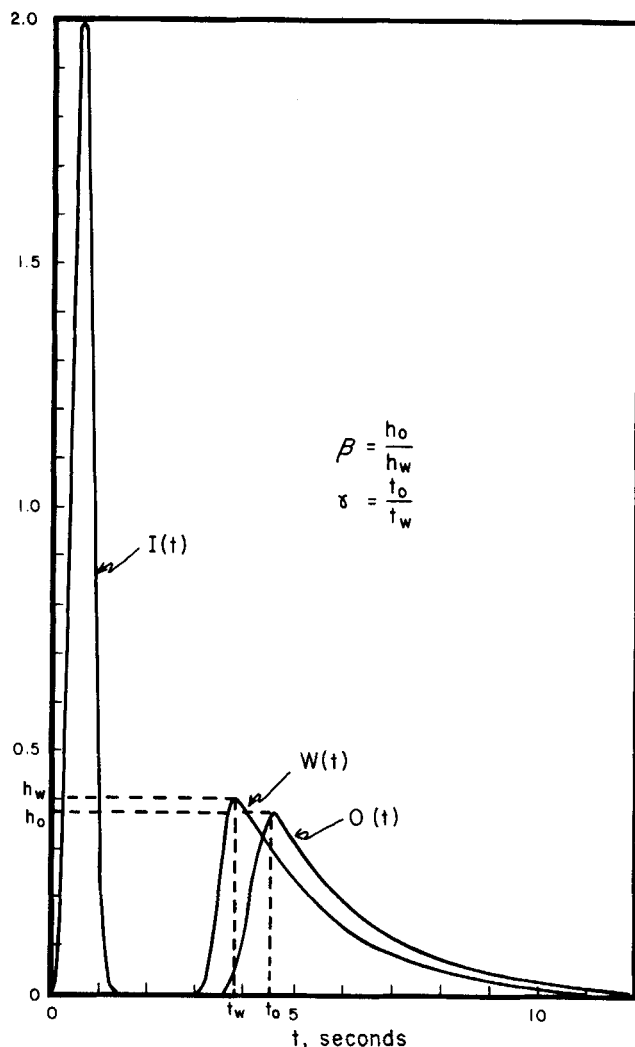


Fig. 4. Input, realistic weighting function [Equations (5) and (9)], and the output given by convolution. Input  $\sigma = 0.2$  s.

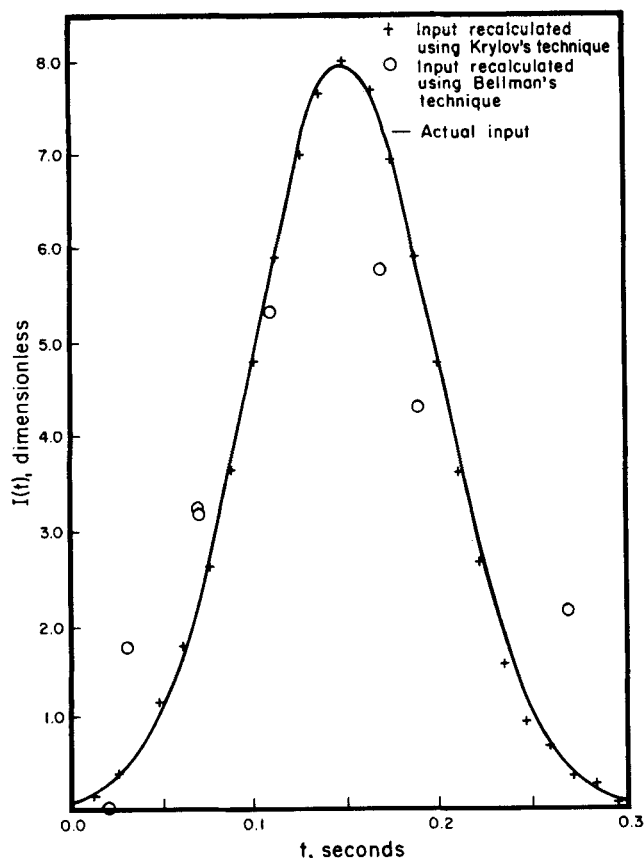


Fig. 5. Simple weighting function: comparison between inputs when numerically transforming the output, for an input  $\sigma = 0.5$  s ( $\alpha = 0.3$  s,  $\beta = 0.93$ ).

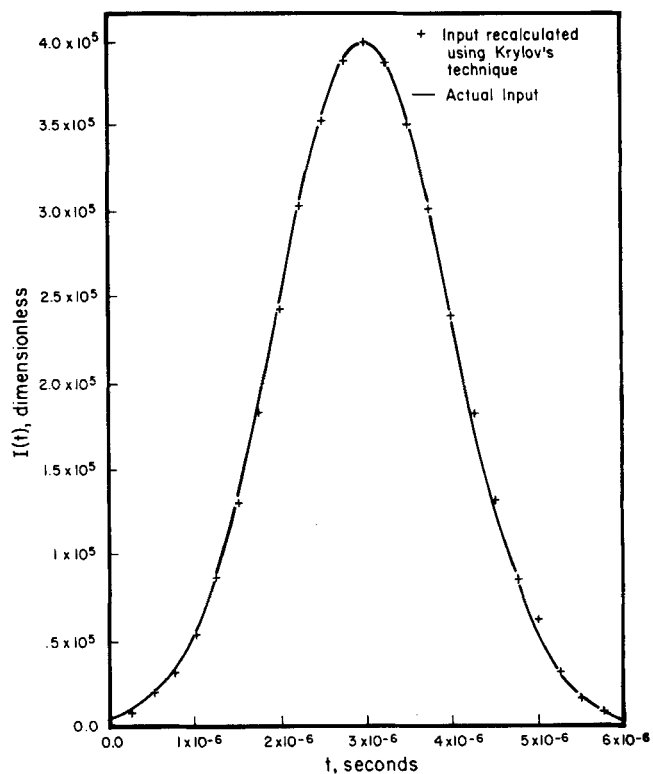


Fig. 6. Simple weighting function: comparison between inputs when numerically transforming the output, for an input  $\sigma = 10^{-6}$  s ( $\alpha = 7 \times 10^{-6}$  s,  $\beta = 1.00$ ).

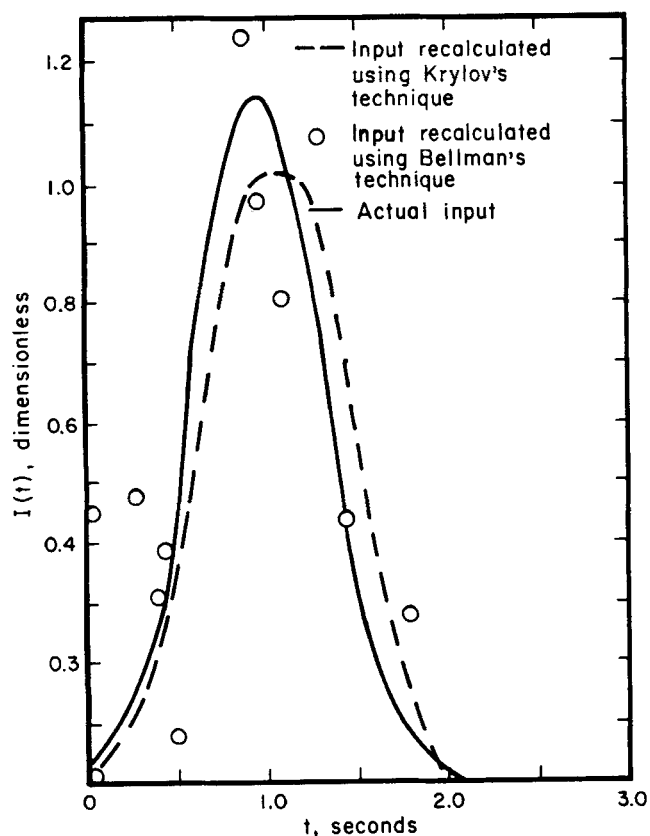


Fig. 7. Realistic weighting function: comparison between inputs when transforming the output numerically for input  $\sigma = 0.35$  s ( $\beta = 1.21$ ,  $\gamma = 0.76$ ).

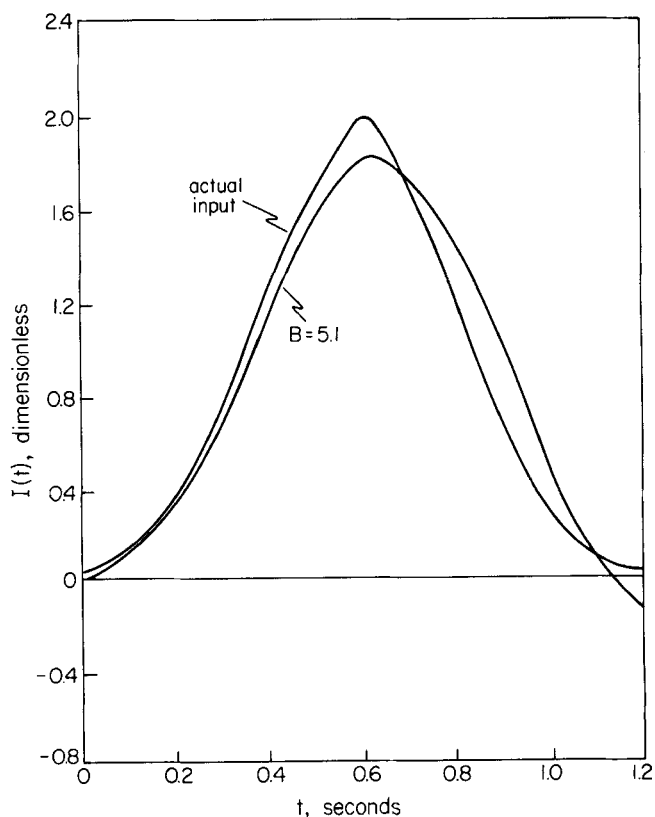


Fig. 8. Realistic weighting function: comparison between inputs when transforming the output numerically for input  $\sigma = 0.2$  s ( $\beta = 1.09$ ,  $\gamma = 0.84$ ).

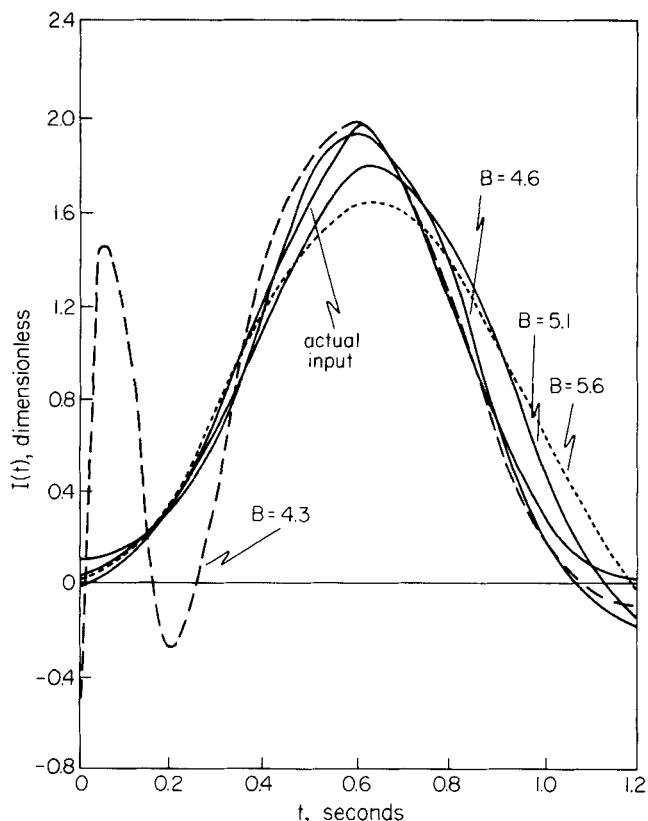


Fig. 9. Realistic weighting function: Comparison between inputs recalculated using different values of estimated time lag,  $B$ .

0.2 s, no agreement was achieved, and so input  $\sigma = 0.2$  s is the limit for Krylov's method.

Special care must be taken when calculating the transform of an output with a time lag. At small times, any disturbance in the function is greatly amplified because of the rapidly decreasing magnitude of  $e^{-pt}$  in the transformation integral. To surmount this difficulty, the numeri-

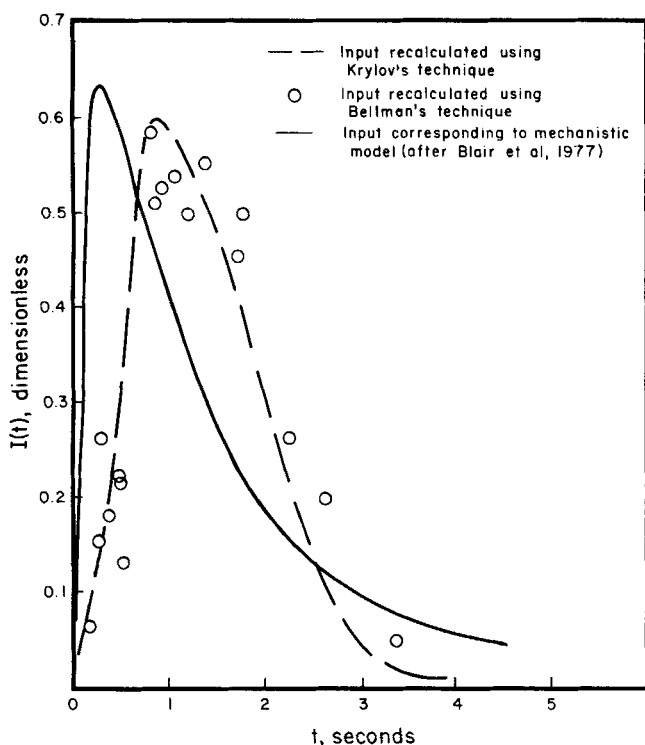


Fig. 10. Analysis of experimental data: Bellman's and Krylov's inversion techniques transforming the experimental output numerically.

cally calculated output was only considered nonzero when the integral was larger than 1% of the final value.

It is important to note that Krylov's method failed when the apparent time lag generated by the weighting function was used. When a larger time lag was used, the method produced more reasonable results. Figure 9 shows the results obtained using Krylov's method with different time lags. The apparent time lag (that is, that corresponding to appearance of 1% of the area of the total output signal) was 3.6 s, and all the curves are shifted to initial time zero in order to make the comparison with the given input possible.

It can be observed that the best agreement with the original input is obtained when the apparent time lag is overestimated by 1.5 s. Higher values do not alter the results much, while lower values drastically change the shape of the recalculated functions.

#### Reduction of Experimental Data

The data reduction method was applied to an experimental data set for which an input function had been estimated through the use of a mechanistic model (Blair et al., 1977). The data set used was denoted WYODAK #11 in that publication.

The real time lag of the output was not measured. In order to overcome that problem, an arbitrary large time lag was assumed, and the input function was obtained. The effect of the large time lag was to shift the input so that it started at some positive value of time.

Results obtained through the application of this method are shown in Figure 10, where the calculated input function was assumed to begin at the origin. Both inversion techniques give results which agree very well with each other and reasonably well with those obtained by Blair et al. (1977). Note that the continuous function that can be derived using Krylov's technique does not represent the curve which would best seem to fit the points obtained using Bellman's technique.

#### NOTATION

$B$	estimated time lag, s.
$D_e$	dispersion coefficient, $\text{cm}^2 \text{s}^{-1}$
$D_N$	dispersion parameter ( $= \frac{D_e}{uL}$ )
$f(t)$	function in time domain
$F(p)$	Laplace Transform of $f(t)$
$i$	$\sqrt{-1}$
$I(t)$	input function, $\text{s}^{-1}$
$L$	capillary length, cm
	dispersion parameter ( $= \frac{1}{2D_N}$ )
$O(t)$	output function, $\text{s}^{-1}$
$p$	complex variable in Laplace Space
$t$	time, s
$\bar{t}$	mean of Normal Distribution, Eq. 5, s.
$\bar{u}$	mean velocity in capillary, $\text{cm s}^{-1}$
$W(t)$	weighting function, $\text{s}^{-1}$
$W(p)$	transfer function, Laplace Transform of $W(t)$
Greek Letters	
$\alpha$	defined in Fig. 3, s.
$\beta$	defined in Fig. 3, see text.
$\beta_1$	defined in Eq. 11.
$\gamma$	defined in Fig. 4, see text.
$\delta$	defined in Eq. 13.
$\theta$	defined in Eq. 12.
$\sigma$	variance of Normal Distribution, Eq. 5, s.
$\tau_1$	mean residence time in well stirred tank, s.
$\tau_2$	mean residence time in capillary, s.

## LITERATURE CITED

- Bellman, R. E., H. H. Kagiwada, R. E. Kalaba, and M. C. Prestrud, *Invariant Imbedding and Time-Dependent Transport Processes*, American Elsevier, New York (1964).
- Bellman, R. E., R. E. Kalaba, and J. A. Lockett, *Numerical Inversion of the Laplace Transform: Applications to Biology, Economics, Engineering and Physics*, American Elsevier, New York (1966).
- Blair, D. W., J. O. L. Wendt, and W. Bartok, "Evolution of Nitrogen and other Species during Controlled Pyrolysis of Coal," Sixteenth Symposium (International) on Combustion, p. 475, The Combustion Institute, Pittsburgh, Pa. (1977).
- Filon, L. N. G., "On a Quadrature Formula for Trigonometric Integrals," *Proc. Royal Soc. Edinburgh*, 49, 38 (1928).
- Hahn, W. A., "Use of the Laplace Transform for the Time Resolution of Rapid Processes Applied to Coal Volatilization," M.S. thesis, Univ. Ariz., Tucson (1977).
- , and F. P. Plachco, "Solid-Liquid Extraction in Co- or Countercurrent," *Lat. Am. J. Chem. Eng. Appl. Chem.*, 7, 3 (1977).
- Krylov, V. I., and N. S. Skoblya, *Handbook of Numerical Inversion of Laplace Transforms*, IPTS Press, Wiener Bindery, Ltd., Jerusalem, Israel (1969).
- Marquardt, D. G., *J. Soc. Indust. Appl. Math.*, 3, 431 (1963).
- Seinfeld, J. M., and L. Lapidus, *Mathematical Models in Chemical Engineering*, Vol. 3, Prentice-Hall, Englewood Cliffs, N.J. (1974).
- Sy, F., and E. N. Lightfoot, "Transient Creeping Flow Around Fluid Spheres," *AIChE J.*, 17, 177 (1971).
- Wen, C. Y., and L. T. Fan, *Models for Flow Systems and Chemical Reactors*, p. 130ff, Marcel Dekker, New York (1975).

Manuscript received August 8, 1977; revision received June 30, and accepted July 19, 1978.

## JOURNAL REVIEW

# Hydrodynamics and Solid-Liquid Contacting Effectiveness in Trickle-Bed Reactors

A. GIANETTO, G. BALDI, V. SPECCHIA, and S. SICARDI

Istituto di Chimica Industriale,  
Politecnico, 10100 Torino, Italy

The term trickle-bed reactor usually means a reactor in which a liquid phase and a gas phase flow concurrently downward through a bed of catalytic pellets.

Trickle-bed reactors or similar apparatuses are used in the chemical, petrochemical, and petroleum industries, as well as in the field of wastewater treatment (trickling filters).

Considerable attention has therefore been recently directed to their fundamental mechanisms. These are rather complicated, owing to the three phases involved.

The subject as a whole has been reviewed in three papers (Satterfield, 1975; Hofmann, 1977; Hofmann, 1978); in addition, Laurent et al. (1974) and Charpentier (1976) have reviewed gas-liquid mass transfer in packed beds.

Most recent works on trickle-bed reactors deal with their hydrodynamics, modeling, and solid-liquid contacting effectiveness. Although in these works comparisons are made between the results obtained from different sources, a more extensive, critical analysis of these three topics seems worthwhile.

## HYDRODYNAMICS

The hydrodynamics studies considered in this section concern the flow regimes, liquid distribution on the pack-

ing, pressure drop, and liquid holdup. The following parameters must be considered: gas and liquid flow rates, physical properties of the liquid phase, foaming characteristics of the system, and packed-bed geometry.

## Hydrodynamic Regimes

**Two-phase flow regimes.** Many studies have been carried out for two-phase concurrent downward flow with nonfoaming systems (Larkins et al., 1961; Weekman and Myers, 1964; Sato et al., 1973; Charpentier and Favier, 1975; Midoux et al., 1976; Chou et al., 1976; Specchia and Baldi, 1977). For an air-water system at low liquid flow rates ( $L < 3$  to  $5 \text{ kg/m}^2\text{s}$ ), a gas continuous channeled or trickling flow occurs at low gas flow rates; then, by increasing the gas flow rate, a spray flow appears.

At  $L$  between 5 and  $35 \text{ kg/m}^2\text{s}$ , on increasing the gas flow rate, gas continuous channeled flow, pulsing flow, and spray flow occur in succession.

When  $L > 35 \text{ kg/m}^2\text{s}$ , and the gas flow rate is low, a dispersed bubble flow can be observed, followed by a pulsing flow when the gas flow rate is increased.

The hydrodynamic regimes set up in a packed bed when foam appears have been defined by Charpentier and Favier (1975) and Midoux et al. (1976). Trickling flow, foaming flow, foaming-pulsing flow, pulsing flow, and spray flow can be observed.